

Ferromagnetic Quantum Criticality in the Quasi-One-Dimensional Heavy Fermion Metal YbNi_4P_2

C Krellner, S Lausberg, A Steppke, M Brando, L Pedrero, H Pfau, S Tencé, H Rosner, F Steglich, and C Geibel

Max Planck Institute for Chemical Physics of Solids, D-01187 Dresden, Germany

E-mail: krellner@cpfs.mpg.de

Abstract. We present a new Kondo-lattice system, YbNi_4P_2 , which is a clean heavy-fermion metal with a severely reduced ferromagnetic ordering temperature at $T_C = 0.17\text{K}$, evidenced by distinct anomalies in susceptibility, specific-heat, and resistivity measurements. The ferromagnetic nature of the transition, with only a small ordered moment of $\sim 0.05\mu_B$, is established by a diverging susceptibility at T_C with huge absolute values in the ferromagnetically ordered state, severely reduced by small magnetic fields. Furthermore, YbNi_4P_2 is a stoichiometric system with a quasi-one-dimensional crystal and electronic structure and strong correlation effects which dominate the low temperature properties. This is reflected by a stronger-than-logarithmically diverging Sommerfeld coefficient and a linear-in- T resistivity above T_C which cannot be explained by any current theoretical predictions. These exciting characteristics are unique among all correlated electron systems and makes this an interesting material for further in-depth investigations.

Phase transitions are one of the most fascinating phenomena and a central topic in solid-state physics. While classical phase transitions driven by thermal fluctuations have been extensively studied, the current interest is on continuous quantum phase transitions which occur at zero temperature and are caused by collective quantum fluctuations between competing ground states [1]. Namely, the emergence of intriguing new states of matter at such a quantum critical point (QCP) was explored in great detail in Lanthanide-based heavy-fermion systems [2, 3, 4, 5, 6]. However, despite these studies over more than two decades, no $4f$ -based material has been found with a ferromagnetic (FM)-to-paramagnetic quantum phase transition. The reason for this lapse remains hotly debated [7, 8, 9]. Here, we present a new heavy-fermion metal, YbNi_4P_2 , which indeed presents FM quantum criticality above a low-lying FM transition temperature.

Intermetallic pnictides have recently become a focus in the solid state physics community as a result of the discovery of high-temperature superconductivity in the RFeAsO (R = rare earth) and AFe_2As_2 (A = alkali metal) systems with different substitutions (for a review see e.g. Ref. [10]). While these compounds present a pronounced quasi-two-dimensional character, the pnictides crystallising in the ZrFe_4Si_2 structure type are quasi-one-dimensional and have been poorly investigated [11, 12, 13]. In Fig. 1a we present the tetragonal ZrFe_4Si_2 structure type ($P4_2/mnm$) of YbNi_4P_2 which can be viewed as isolated chains (along the c direction) of edge-connected Ni tetrahedra, with adjacent chains linked by Ni-Ni bonds between corners of the tetrahedra. The Yb atoms are located in the channels between these Ni tetrahedral chains. The quasi-one-dimensional character in the Yb and in the Ni network, as well as the geometrical frustration between neighboring Yb chains which are shifted by $c/2$, are prone to cause strong quantum fluctuations if Yb is magnetic (Yb^{3+}).

Previously, only a susceptibility curve at high temperatures of an impure YbNi_4P_2 sample was reported by Deputier *et al.* [14]. These authors suggested magnetic Yb^{3+} ions and a non-magnetic contribution of the “ Ni_4P_2 ” sublattice revealed by weak Pauli paramagnetism in the reference compound YNi_4P_2 , in contrast to the first measurements by Chikhrij *et al.* [15] which suggest a ferromagnetically ordered sublattice above room temperature, most probably due to Ni impurity phases. We succeeded in preparing single-phase YbNi_4P_2 polycrystals. Our susceptibility measurements, $\chi(T)$, indicate a clear Curie-Weiss behaviour between 50 and 400 K with a Weiss temperature, $\Theta_W = 35$ K, and an effective moment, $\mu_{\text{eff}} = 4.52 \mu_B$, due to magnetic Yb^{3+} ions, thus supporting the absence of a Ni moment. The lattice parameters $a = 7.0565(2)$ Å and $c = 3.5877(1)$ Å refined by simple least squares fitting agree well with the reported structure data [16]. A complete structure refinement based on tiny single crystals is given in the Appendix B.

To gain insight into the electronic structure of YbNi_4P_2 , we performed band structure calculations of the “ Ni_4P_2 ” sublattice. For this purpose, the $4f^{13}$ electrons are frozen as core states and are not allowed to hybridise with the conduction electrons as the strong Coulomb correlations of the Yb $4f$ electrons would give incorrect results in the mean-field approximation. Two main results can be inferred from the uncorrelated band

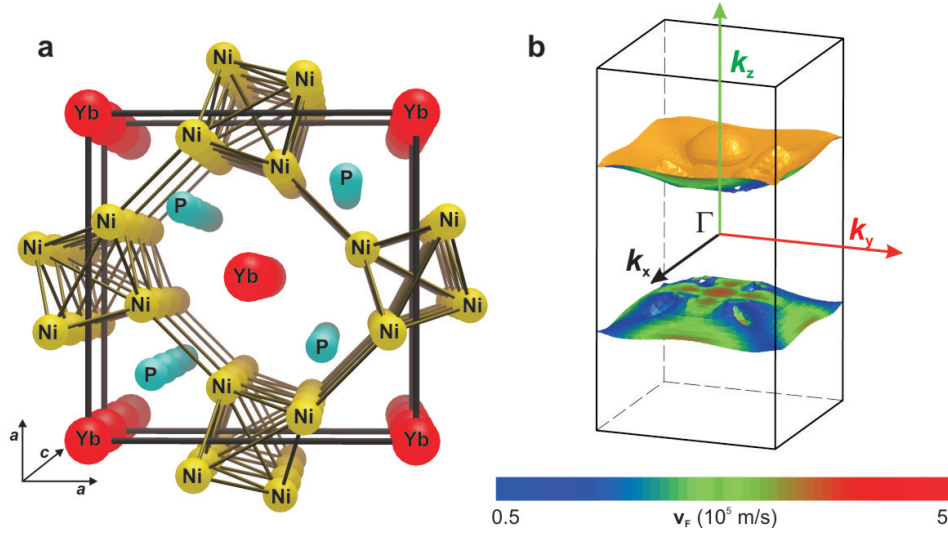


Figure 1. Quasi-one-dimensional crystal and electronic structure of YbNi_4P_2 .

a, Stereoscopic view of the tetragonal crystal structure along c with the Yb chains located in the channels between chains of edge-connected Ni tetrahedra. Details of the structural refinement of our samples are given in the Appendix B.

b, Topology of one of the uncorrelated Fermi surfaces with the most pronounced one-dimensional character manifested in two nearly flat sheets, well separated along k_z . Note that the viewing direction is rotated by 90° compared to the crystal structure. The size of the Fermi velocity, v_F , of the mainly Ni-3d states dominating the density of states at E_F is colour-coded.

structure: First, the three main Fermi surfaces have a predominantly one-dimensional (1D) character: The most prominent one is visualised in Fig. 1b with two nearly flat sheets (well separated along k_z), which is typical for a 1D system in real space. Therefore, not only the crystal structure, but also the electronic structure suggest that YbNi_4P_2 is a quasi-1D system, unique among Kondo-lattice systems. Second, spin-polarised calculations clearly demonstrate the absence of Ni-related magnetism in YbNi_4P_2 , although the main contributions to the density of states at the Fermi energy, E_F , result from Ni-3d states.

The temperature dependence of the resistivity, $\rho(T)$, and the Seebeck coefficient, $S(T)$, between 2 and 300 K (Fig. 2) evidence YbNi_4P_2 as a Kondo lattice with strong interactions between $4f$ and conduction electrons. $\rho(T)$ decreases linearly down to 50 K with a room temperature value of $\rho_{300\text{K}} \cong 120 \mu\Omega\text{cm}$, before dropping rapidly below 20 K due to the onset of coherent Kondo scattering. The correspondingly large residual resistivity ratio, $\rho_{300\text{K}}/\rho_0 = 50$, reveals a long electronic mean free path at low T , which demonstrates the high quality of our polycrystalline sample. Assuming that the linear decrease down to 50 K dominantly results from phonon scattering, the magnetic part of the resistivity reveals a typical Kondo maximum around 30 K. The presence of strong hybridisation between the $4f$ and the conduction electrons in YbNi_4P_2 is further supported by thermopower measurements (see Fig. 2b). $S(T)$ is negative within

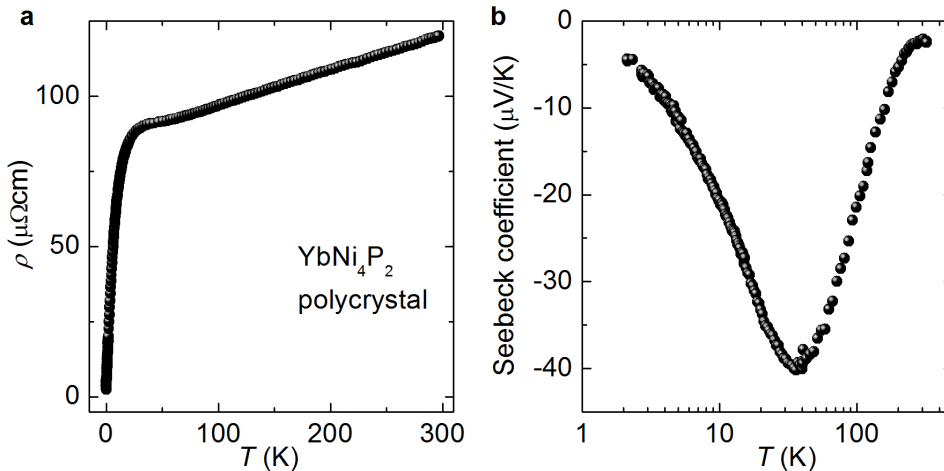


Figure 2. YbNi_4P_2 : A metallic Kondo lattice.

a, The temperature dependence of the resistivity is overall metallic with a pronounced drop below 30 K, marking the onset of coherent Kondo scattering. The high residual resistivity ratio, $\rho_{300\text{K}}/\rho_0 = 50$, demonstrates that our polycrystalline sample is very clean.

b, The temperature dependence of the Seebeck coefficient shows a distinct minimum at 35 K, characteristic for Yb-based Kondo lattices. The large absolute values near this minimum are commonly ascribed to a strongly energy-dependent quasiparticle density of states at E_F .

the whole temperature range investigated, a fact that is well established in Yb-based Kondo lattices. Moreover, $S(T)$ presents a pronounced minimum at 35 K with absolute values as high as $40 \mu\text{V}/\text{K}$. Extrema in $\rho(T)$ and $S(T)$ originate from Kondo scattering on the ground and the excited crystal electric field (CEF) levels [17]. Since the CEF scheme of YbNi_4P_2 is presently unknown, a reliable estimate of the Kondo energy scale, T_K (for the lowest-lying CEF Kramers doublet), can only be obtained by means of the magnetic entropy calculated from the specific heat data, discussed below. At 4 K, the entropy reaches $0.5R \ln 2$, establishing a doublet ground state with $T_K \cong 8 \text{ K}$.

We now turn to the exciting low-temperature properties of YbNi_4P_2 presented in Fig. 3. Below $T = 10 \text{ K}$, the a.c. susceptibility, χ , increases and nearly diverges towards $T_C = 0.17 \text{ K}$ where the $4f$ moments undergo a FM phase transition. The temperature and magnetic field dependence of χ are distinctive for a ferromagnetically ordered material (see Fig. 3a). The FM nature of the magnetic phase is one of our key results since the majority of the presently known Kondo lattices order antiferromagnetically. Most prominent are the huge absolute values of χ in zero magnetic field. To assess the magnitude of the divergence at T_C , we scaled the right hand ordinate of Fig. 3a to the dimensionless volume susceptibility, e.g., $\chi_{vol} = \chi_{mol}/V_{mol}$ with the molar volume, $V_{mol} = 53.8 \times 10^{-6} \text{ m}^3/\text{mol}$. To better compare this with the susceptibility of prototypical ferromagnets as e.g. iron, we need to consider two more facts. First, the ferromagnetically ordered moment in YbNi_4P_2 is a factor of 20 times smaller (see below) and second, the density of the magnetic Yb ions is 7.5 times lower than in iron.

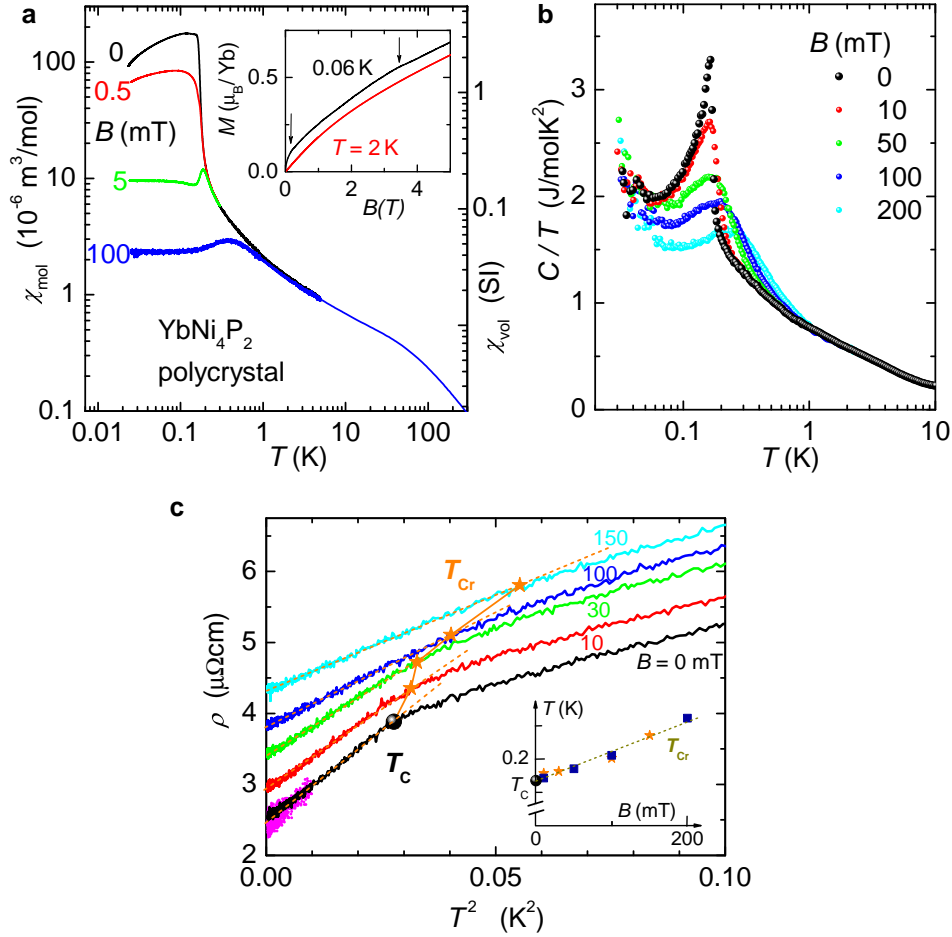


Figure 3. Low-lying ferromagnetic transition at $T_C = 0.17$ K in YbNi_4P_2 .

a, Temperature-dependent a.c. susceptibility, $\chi_{mol}(T)$, at selected magnetic fields reveals a FM phase transition at T_C with very high absolute values. The right hand ordinate is divided by the molar volume, representing the dimensionless volume susceptibility in SI units. In the inset, the field dependence of the magnetisation below (black line) and above (red line) T_C is shown. The arrow on the left hand side indicates the step-like increase due to the small ordered FM moment, $M_{\text{Ord}} \cong 0.05 \mu_B$, obtained by extrapolating the linear $M(H)$ curve between 0.1 and 0.2 T to zero field. The right hand arrow marks an anomaly at higher field either representing the rotation of the FM moments along the magnetic hard direction or the complete suppression of the Kondo screening.

b, Low-temperature specific heat plotted as C/T versus T on a logarithmic scale at zero and low values of the applied magnetic field without subtraction of any hyperfine nor phononic contribution. A sharp λ -type anomaly at T_C confirms the second-order phase-transition and the high quality of our sample. With increasing field, the peak broadens and transforms into a Schottky-type anomaly with a maximum at T_{Cr} .

c, Temperature dependence of the resistivity plotted as a function of T^2 , dashed lines indicate the formation of a Landau-Fermi liquid ground state. For the sake of clarity, the different curves for $B > 0$ are shifted by $0.5 \mu\Omega\text{cm}$, respectively. For the zero field curve, we additionally present data measured with very low excitation current but less resolution (magenta curve) to demonstrate the absence of heating effects above 0.07 K. The zero-field transition at T_C (black symbol) becomes a crossover at T_{Cr} (orange stars) in finite field, shown together in the inset with the specific heat crossover temperatures (blue squares) in a B - T -phase diagram.

Therefore, the scaled relative permeability for YbNi_4P_2 is as high as ~ 500 , very similar to iron. The fact that the magnetic ordering temperature of the Yb moments is so strongly reduced results primarily from the pronounced Kondo interactions. Further evidence for ferromagnetism comes from the very pronounced field dependence of the susceptibility which is suppressed by a factor of two, applying a small field of $B = 0.5$ mT. This makes an AFM or helical order rather unlikely. However, we cannot completely exclude a magnetic ordering vector with a very tiny q , but also in such a case the FM interaction would be the most dominant one. For $B \geq 5$ mT, a broad maximum develops in $\chi(T)$, which shifts to higher temperatures with increasing fields due to the energetic stabilisation of the FM ground state in a magnetic field. In the inset of Fig. 3a we present the magnetisation data below and above T_C obtained from the same sample, confirming the FM nature of the magnetic transition. At 60 mK, the magnetisation is strongly nonlinear and increases steeply with field below $B = 150$ mT due to a small ordered FM moment of $M_{\text{ord}} \cong 0.05 \mu_B$, followed by a second kink at $B = 3.5$ T, which either represents the rotation of the FM moments along the magnetic hard direction (perpendicular to the direction of the FM moment) or the complete suppression of the Kondo screening. Above T_C , both anomalies are absent and the polarised moment amounts to $M \cong 0.6 \mu_B$ at $B = 5$ T. More detailed magnetisation measurements at low fields are presented in the Appendix A.

Specific heat data, shown in Fig. 3b, strongly confirm that YbNi_4P_2 is a magnetically ordered heavy-fermion system. A sharp λ -type anomaly is observed at T_C , establishing a second-order phase transition into the FM phase. Well below T_C , a huge Sommerfeld coefficient, $\gamma_0 \cong 2000$ mJ/molK², reflects the existence of heavy quasiparticles with an electronic mass two to three orders of magnitude bigger than the bare electron mass. Below 50 mK, the scattering of the data points significantly increases, preventing a more accurate determination of the Sommerfeld coefficient. Remarkably, C/T is larger below T_C than above the FM ordering, indicating strong fluctuations within the ferromagnetically ordered state, similar to the antiferromagnetic (AFM) phase in YbRh_2Si_2 [18]. Integrating C/T over temperature reveals an entropy gain associated with the anomaly at T_C of only about $0.02R \ln 2$. This is in accordance with the small value of the ordered moment derived from our magnetisation data and provides evidence for rather weak FM order in YbNi_4P_2 .

The onset of magnetic order is further established by the freezing out of spin-disorder scattering, i.e., a distinct reduction of the electrical resistivity at T_C , presented as ρ vs. T^2 in Fig. 3c. Below T_C , the resistivity follows a straight line down to the lowest measured temperatures, i.e. $\rho(T) = \rho_0 + AT^2$ with $\rho_0 \cong 2.5 \mu\Omega\text{cm}$ and $A \cong 52 \mu\Omega\text{cm}/\text{K}^2$. Therefore, all measured quantities present the hallmarks of a Landau-Fermi-liquid ground state within the FM ordered phase and can be characterised by the $T \rightarrow 0$ limits of the susceptibility, χ_0 , Sommerfeld coefficient of the electronic specific heat, γ_0 , and the resistivity coefficient A . The so-called Kadowaki-Woods ratio, A/γ_0^2 , amounts to approximately $13 \mu\Omega\text{cmK}^2\text{mol}^2/\text{J}^2$, close to the universal value of $10 \mu\Omega\text{cmK}^2\text{mol}^2/\text{J}^2$ for heavy-fermion compounds [19]. The Sommerfeld-Wilson ratio,

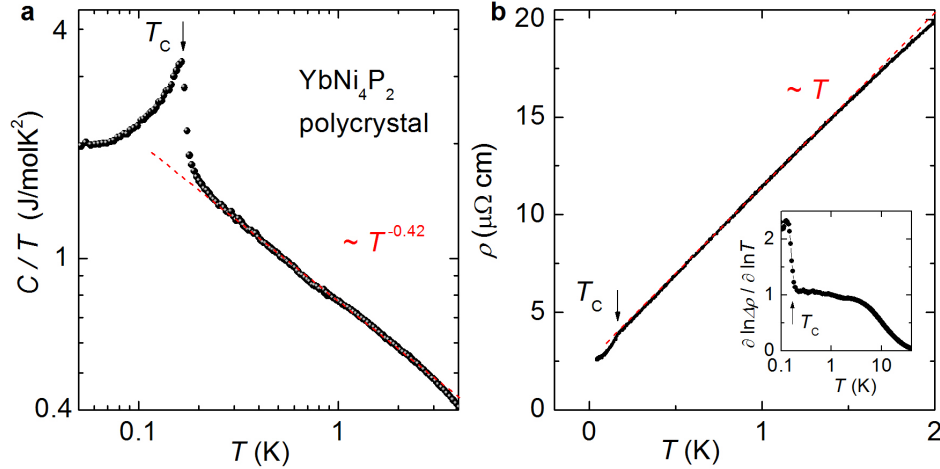


Figure 4. Pronounced non-Fermi-liquid behaviour above T_C at $B = 0$.

a, The temperature dependence of the zero-field specific heat divided by temperature in a double logarithmic representation clearly reveals a power law divergence, $C/T \propto T^{-0.42}$, indicated by the red dashed line.

b, Linear-in- T resistivity in zero field over more than a decade in temperature. A pronounced drop at T_C precedes a T^2 law within the ordered phase. The temperature dependence of the resistivity exponent, defined as the derivative of $\ln[\Delta\rho(T)] = \ln[\rho(T) - \rho_0]$ with respect to $\ln T$, is presented in the inset.

$W = \pi^2 k_B^2 / (\mu_0 \mu_{\text{eff}}^2) \cdot \chi_0 / \gamma_0$ with $\mu_{\text{eff}} \cong 2 \mu_B$, is found to be huge compared to all other heavy fermion systems where typically values between 1 and 5 are observed [20]. In YbNi_4P_2 , a giant value of W is observed within the ferromagnetically ordered state ($W_{T \rightarrow 0} \cong 350$) and W is still substantially enhanced well above T_C , $W_{T=0.3\text{K}} \cong 20$. This leads further support to very strong FM quantum fluctuations in YbNi_4P_2 .

The effect of an applied magnetic field is similar for all presented quantities: Already a small ($\cong 10$ mT) magnetic field extends the Landau-Fermi-liquid ground state to higher temperatures and is accompanied by a reduction of the effective mass reflected in decreased values of γ_0 , A , and χ_0 . The field-stabilised FM state is characterised by broad crossover maxima at T_{Cr} in $\chi(T)$ and $C(T)/T$, respectively, as the Yb-moments get polarised in the external field at higher temperatures (see inset of Fig. 3c). Therefore, the system is tuned away from the QCP, in striking contrast to AFM systems, where an ordered system may be field-tuned through the QCP [3, 21, 22].

Having established the proximity of YbNi_4P_2 to a FM QCP we now turn to the quantum critical regime and address the distinct deviations from the predictions of Landau-Fermi-liquid (LFL) theory above T_C . They are most pronounced in zero magnetic field, where YbNi_4P_2 is closest to the QCP. Remarkably, the specific-heat coefficient diverges stronger than logarithmically below $T = 3$ K with a power law $C/T \propto T^{-0.42}$ down to 0.2 K. At this temperature the classical fluctuations of the FM order parameter set in (see Fig. 4a). Above $T = 1$ K, there might be a crossover from a power-law to a logarithmic divergence up to $T = 7$ K, better seen in the semi-logarithmic

plot of C/T vs. T in Fig. 3b. The resistivity follows a linear-in- T dependence for $T > T_C$, presented in Fig. 4b, with a tendency to sub-linear behaviour above $T = 2$ K. For a more quantitative analysis of the resistivity exponent, we consider the logarithmic derivative, $\partial \ln(\rho - \rho_0)/\partial \ln T$. As displayed in the inset of Fig. 4b, $\partial \ln(\rho - \rho_0)/\partial \ln T$ remains within the value 1.0 ± 0.1 over more than one decade in temperature above T_C before dropping above 5 K.

These strong deviations from LFL behaviour along with the low-lying FM ordering have very general implications for our current understanding of quantum phase transitions. While numerous AFM Kondo systems have been tuned towards a QCP by variation of pressure, doping or magnetic field, appropriate candidates for the study of FM QCPs are extremely rare [3]. Starting deep inside the localised moment regime in Ce-based ferromagnets, the increase of the Kondo interaction with pressure typically leads to an AFM ground state before the QCP is reached [7]. In disordered FM $4f$ systems a peculiar Kondo-cluster-glass state was found, preventing the study of FM quantum criticality [23]. On the other hand, in clean itinerant FM $3d$ systems, it is established that no QCP exists, rather the FM transition always ends at a classical critical point (at finite T) where a first-order phase transition occurs [8, 24]. However, disorder can lead to weak signatures of FM quantum criticality as observed in various $3d$ alloy series [25, 26, 27], which theoretically could be explained by disorder-induced rounding effects [28]. Therefore, YbNi_4P_2 represents the first clean example of FM quantum criticality above a low-lying FM transition, permitting the examination of existing and the development of new theoretical predictions for the temperature dependencies of the relevant physical parameters at a FM QCP. Most theoretical work has been done in systems where the vanishing magnetism can be described within the framework of itinerant spin fluctuation theories [3]. However, our observed power laws in $C(T)/T$ and $\rho(T)$ above T_C deviate strongly from these theoretical descriptions. Presently, we cannot distinguish whether these deviations result from the quasi-one dimensionality of YbNi_4P_2 , for which no calculations have been performed, or whether YbNi_4P_2 is situated close to a local QCP, where the FM transition is accompanied by a localisation-delocalisation transition of the f electrons. The local QCP scenario is well established for YbRh_2Si_2 [29] which presents AFM order below $T_N = 72$ mK, but nonetheless shows strong FM fluctuations in wide parts of its phase diagrams [30, 31]. We note that in YbRh_2Si_2 , $C(T)/T$ also follows a stronger-than-logarithmically divergence below 300 mK and a linear-in- T resistivity [32]. Furthermore, a sharp λ -type transition into the antiferromagnetically ordered phase and a strongly enhanced Sommerfeld coefficient below T_N were similarly observed for YbRh_2Si_2 [33]. Future work has to be undertaken to tune YbNi_4P_2 towards the non-magnetic side of the QCP. Negative chemical pressure achieved by As substitution on the P site might be the most promising route as the stoichiometric YbNi_4As_2 forms in the same crystal structure but with non-magnetic Yb^{2+} ions [14] due to the much larger volume of the unit cell.

To conclude, we have discovered a new heavy-fermion Kondo-lattice system with several features that are unique among strongly correlated $4f$ systems. First, both the

crystal and the electronic structure of YbNi_4P_2 are quasi-one-dimensional, originating in distinct quantum fluctuations at low temperatures. Second, YbNi_4P_2 undergoes a well-defined ferromagnetic phase transition of second order at $T_C = 0.17$ K, growing out of a strongly correlated Kramers doublet ground state with a Kondo temperature, $T_K \cong 8$ K. Due to the dominant Kondo screening only a tiny ferromagnetically ordered moment ($M_{\text{ord}} \cong 0.05 \mu_B$) with a substantially reduced T_C is observed. The ferromagnetism is evidenced by a diverging susceptibility at T_C with huge absolute values comparable to established ferromagnets. The $4f$ spins remain strongly fluctuating down to the lowest measured temperatures, leading to a large Sommerfeld coefficient, $\gamma_0 \cong 2000$ mJ/molK², within the ordered phase. Above T_C , a remarkable power-law divergence of the specific heat, $C/T \propto T^{-0.42}$, and a linear-in- T resistivity are observed over more than a decade in temperature. Therefore, YbNi_4P_2 is the first clean system situated in the close vicinity of a ferromagnetic quantum critical point with the lowest lying T_C ever observed among correlated systems. These ferromagnetic quantum fluctuations which dominate the thermodynamic and transport properties well above T_C cannot be explained within any current theoretical framework. Furthermore, YbNi_4P_2 is a highly stoichiometric system and has the potential to become the prototype of a ferromagnetic quantum critical material.

Acknowledgements

We sincerely thank Ralf Weise, N. Caroca-Canales, and C. Bergmann for assistance in sample preparation. Valuable discussions with M. Baenitz, S. Friedemann, A. Haase, A. Jesche, S. Kirchner, H.-H. Klauß, R. Küchler, N. Mufti, M. Nicklas, R. Sarkar, J. Spehling, O. Stockert, U. Stockert, and S. Wirth are gratefully acknowledged. This work is partially supported through DFG Research Unit 960 and the SPP 1458.

Appendix A. Methods

The polycrystalline samples were prepared by heating a stoichiometric amount of the elements in evacuated quartz ampoules at 1000°C for 24 hrs. The sample was characterised by powder and single crystalline X-ray diffraction experiments presented in detail in the Appendix B. Electronic band structure calculations were done with the full-potential nonorthogonal local-orbital minimum basis scheme FPLO code (version: FPLO 9.00-31) [34]. Within the local spin density approximation, the exchange and correlation potential of Perdew and Wang has been used [35]. The high-temperature measurements of $\rho(T)$, $S(T)$ and $C(T)$, were performed using a commercial Quantum Design PPMS equipped with a ³He option. The magnetisation and d.c. susceptibility measurements above 2 K were conducted using a Quantum Design SQUID VSM. All low-temperature measurements were carried out in ³He/⁴He dilution refrigerators. The a.c. susceptibility was determined at low frequencies with a modulation field amplitude of 15 μ T down to 0.02 K, measured in selected static magnetic fields. Great care was

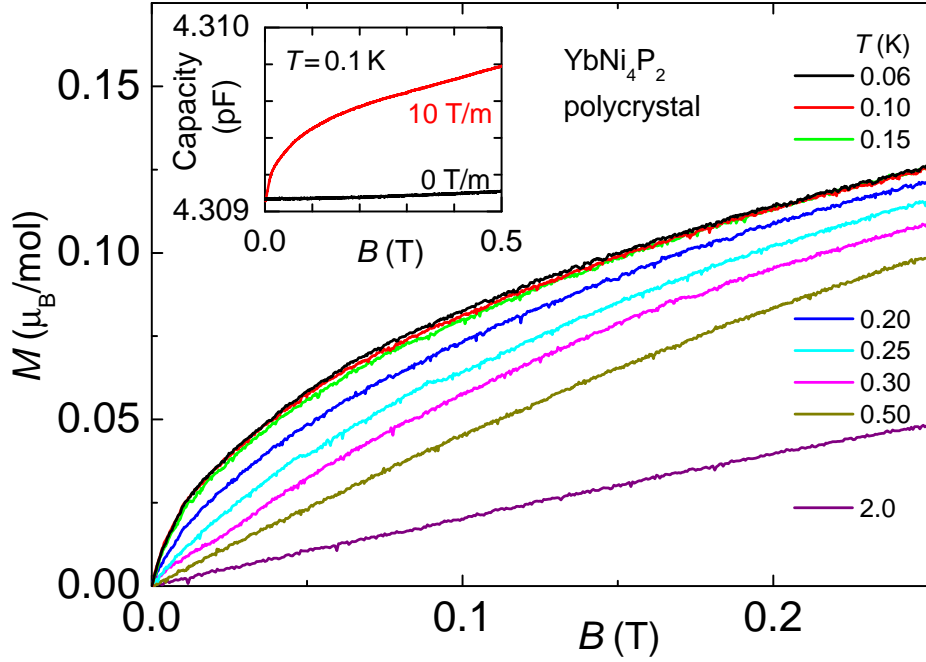


Figure A1. Detailed magnetisation measurements of YbNi_4P_2 at low magnetic fields for various temperatures below and above T_C . The measured capacitance at $T = 0.1$ K with an applied magnetic field gradient ($dB/dz = 10$ T/m, red line) is shown in the inset together with the data measured without the field gradient (black line). The latter serves as a background signal and was subtracted to obtain the presented $M(B)$ curves.

taken to account for remanent fields. Above 2 K, the a.c. susceptibility equals the d.c. susceptibility determined by the SQUID VSM. The specific heat between 0.03 and 1 K was measured utilising a semiadiabatic heat-pulse method with the sample mounted on a silver platform. The electrical resistivity $\rho(T)$ was monitored by a standard four-point lock-in technique at 16.67 Hz down to 0.02 K.

The magnetic field dependence of the magnetisation $M(B)$ was isothermally measured in a high-resolution Faraday magnetometer down to 0.06 K [36]. Background contributions from the sample platform and the torque exerted on the sample have been subtracted and were determined by measuring the capacitance without a magnetic field gradient (black line in the inset of Fig. A1). However, the signal of the sample (red line in the inset of Fig. A1) dominates the field dependence of the capacitance. In the main part of Fig. A1, more detailed $M(B)$ curves are presented in addition to the data in the inset of Fig. 3a. Below T_C , the $M(B)$ curves are nearly temperature independent but decrease strongly above T_C as expected for a FM system.

Appendix B. X-ray diffraction

In Fig. B1, we present the X-ray powder diffraction data of a polycrystalline YbNi_4P_2 sample recorded on an Imaging Plate Guinier Camera (Huber G670, $\text{CuK}\alpha$ radiation,

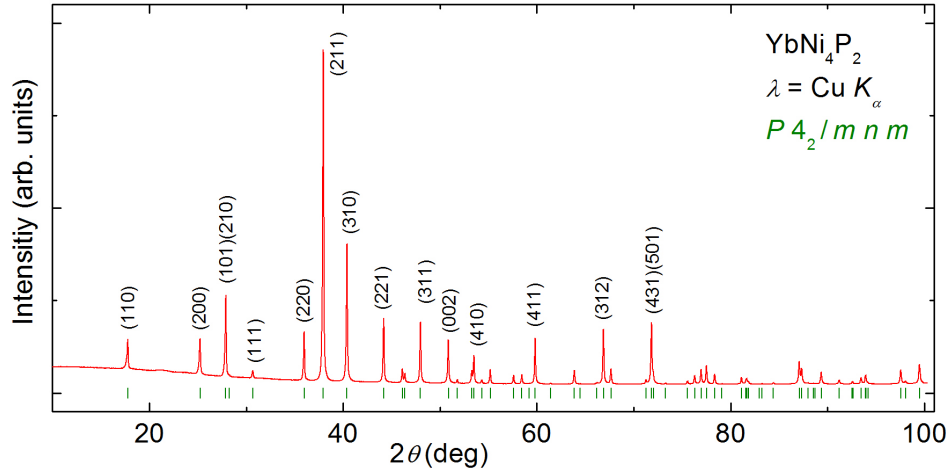


Figure B1. Powder diffraction pattern of YbNi_4P_2 at room temperature. Green lines denote the peak positions for the $P4_2/mnm$ structure type.

$\lambda = 1.5406 \text{ \AA}$). All peaks could be indexed using the ZrFe_4Si_2 structure type (green lines in Fig. B1) confirming the absence of any foreign phase in our sample. Unit cell parameters were refined by a least-squares procedure (program package WinCSD [37]) using the peak positions extracted from powder patterns measured with LaB_6 as an internal standard (not shown).

Furthermore, a complete structural refinement of a small single crystal was carried out on a Rigaku AFC7 diffractometer equipped with a Saturn 724+ CCD detector using $\text{MoK}\alpha$ radiation. The crystallographic information and experimental details of this refinement are presented in Table B1 and were done using the program package ShelX [38]. The structure is in agreement with the literature [16], however, our refinement based on single crystals is more precise than the reported powder data.

These crystallographic data and the refinement corroborate that YbNi_4P_2 is structurally highly ordered without significant crystallographic defects. For the study of quantum critical phenomena at low temperature this is an important conclusion because disorder can often prevail the intrinsic properties particular for materials where the dominating energy scales are small. Furthermore, the excellent stoichiometric quality of our YbNi_4P_2 samples is in nice agreement with the presented physical properties at low temperature, e.g., sharp anomalies at $T_C = 0.17 \text{ K}$ and a large residual resistivity ratio.

Table B1. Crystallographic data and experimental details for the single crystal refinement of YbNi_4P_2 at room temperature.

Crystallographic data: space group $P4_2/mnm$ (no. 136), $a = 7.0565(2) \text{ \AA}$, $c = 3.5877(1) \text{ \AA}$, $V = 178.65(1) \text{ \AA}^3$ (lattice parameters were obtained from powder diffraction data), $Z = 2$, $F(000) = 424$, $U_{13} = U_{23} = 0$, $\rho_{\text{calc}} = 8.73 \text{ g/cm}^3$, $\mu(\text{MoK}\alpha) = 47.24 \text{ mm}^{-1}$, crystal dimensions $20 \times 35 \times 65 \text{ \mu m}^3$.

Collected data: Mo $K\alpha$ radiation ($\lambda = 0.71073 \text{ \AA}$), $2\theta_{\text{max}} = 70^\circ$, 1172 measured reflections, 238 symmetry independent reflections, 226 observed reflections [$I > 2\sigma(I)$], $R_{\text{int}} = 0.040$, 15 parameters, $R(F) = 0.027$, $wR(F^2) = 0.059$, $\text{Goof} = 1.12$, numerical absorption $T_{\text{min}}/T_{\text{max}} = 0.3572$, $\delta\rho_{\text{min}} (\text{max}) = -3.11 (2.13) \text{ e/\AA}^3$.

At.	Site	x/a	y/a	z/c	U_{11}	U_{22}	U_{33}	U_{12}	U_{eq}
Yb	2b	0	0	0.5	0.0070(2)	U_{11}	0.0077(3)	-0.0002(1)	0.0072(2)
Ni	8i	0.3359(1)	0.0840(1)	0	0.0086(4)	0.0077(3)	0.0083(4)	-0.0008(2)	0.0082(2)
P	4g	0.2195(2)	$-x/a$	0	0.0083(5)	U_{11}	0.0076(7)	-0.0004(6)	0.0081(4)

References

- [1] Focus issue. Quantum phase transitions. *Nature Phys.*, 4:167–204, 2008.
- [2] ND Mathur, FM Grosche, SR Julian, IR Walker, DM Freye, RKW Haselwimmer, and GG Lonzarich. Magnetically mediated superconductivity in heavy fermion compounds. *Nature*, 394(6688):39–43, JUL 2 1998.
- [3] GR Stewart. Non-Fermi-liquid behavior in d - and f -electron metals. *Rev. Mod. Phys.*, 73:797–855, Oct 2001.
- [4] T Park, F Ronning, HQ Yuan, MB Salamon, R Movshovich, JL Sarrao, and JD Thompson. Hidden magnetism and quantum criticality in the heavy fermion superconductor CeRhIn_5 . *Nature*, 440:65–68, MAR 2 2006.
- [5] S Friedemann, T Westerkamp, M Brando, N Oeschler, S Wirth, P Gegenwart, C Krellner, C Geibel, and F Steglich. Detaching the antiferromagnetic quantum critical point from the Fermi-surface reconstruction in YbRh_2Si_2 . *Nature Phys.*, 5:465–469, JUL 2009.
- [6] O Stockert, J Arndt, E Faulhaber, C Geibel, HS Jeevan, S Kirchner, M Loewenhaupt, K Schmalzl, W Schmidt, Q Si, and F Steglich. Magnetically driven superconductivity in CeCu_2Si_2 . *Nature Phys.*, 7(2):119–124, FEB 2011.
- [7] S Süllow, MC Aronson, BD Rainford, and P Haen. Doniach Phase Diagram, Revisited: From Ferromagnet to Fermi Liquid in Pressurized CeRu_2Ge_2 . *Phys. Rev. Lett.*, 82:2963–2966, Apr 1999.
- [8] TR Kirkpatrick and D Belitz. Nature of the quantum phase transition in clean itinerant Heisenberg ferromagnets. *Phys. Rev. B*, 67(2):024419, JAN 1 2003.
- [9] SJ Yamamoto and Q. Si. Metallic ferromagnetism in the Kondo lattice. *Proc. Natl. Acad. Sci. USA*, 107(36):15704–15707, SEP 7 2010.
- [10] J Paglione and RL Greene. High-temperature superconductivity in iron-based materials. *Nature Phys.*, 6(9):645–658, SEP 10 2010.
- [11] SI Chikhrij, SV Orishchin, and YB Kuz'ma. New phosphides of rare-earth-metals with the ZrFe_4Si_2 -type structure. *Dopov. Akad. Nauk Ukr. SSR Ser. A*, 7:81–83, 1986.
- [12] JY Pivan, R Guerin, EH El Ghadraoui, and M Rafiq. Tetrahedral Ni_4 clusters in a marcasite-type host structure: The preparation and crystal structure of MNi_4X_2 compounds ($\text{X} = \text{P, As; M} = \text{Zr, Hf, Y, Gd, Tb, Dy, Ho, Er, Tm, Yb, Lu}$). *J. Less Common Met.*, 153:285–292, 1989.
- [13] W Jeitschko, LJ Terbüchte, EJ Reinbold, PG Pollmeier, and T Vomhof. Phosphides and arsenides with the ZrFe_4Si_2 -type structure. *J. Less Common Met.*, 161(1):125–134, JUN 1990.
- [14] S Deputier, O Pena, T Le Bihan, J Y Pivan, and R Guerin. Magnetic properties of the lanthanoid

- nickel arsenides and phosphides LnNi_4X_2 with ZrFe_4Si_2 -type structure. *Physica B*, 233(1):26–36, APR 1997.
- [15] SI Chikhrij, YK Gorelenko, SV Orishchin, RV Skolozdra, and YB Kuz'ma. Anomalous magnetic properties of LnNi_4P_2 phosphides. *Sov. Phys. Solid State*, 33:1556–1557, 1991.
- [16] YB Kuz'ma, SI Chykhrij, and SL Budnyk. Yb-Ni-P system. *J. Alloy. Compd.*, 298(1-2):190–194, FEB 28 2000.
- [17] U Köhler, N Oeschler, F Steglich, S Maquilon, and Z Fisk. Energy scales of $\text{Lu}_{1-x}\text{Yb}_x\text{Rh}_2\text{Si}_2$ by means of thermopower investigations. *Phys. Rev. B*, 77(10):104412, MAR 2008.
- [18] N. Oeschler, S. Hartmann, A. P. Pikul, C. Krellner, C. Geibel, and F. Steglich. Low-temperature specific heat of YbRh_2Si_2 . *Physica B*, 403:1254–1256, APR 1 2008.
- [19] K Kadowaki and SB Woods. Universal relationship of the resistivity and specific-heat in heavy-fermion compounds. *Solid State Commun.*, 58:507–509, MAY 1986.
- [20] Z Fisk, HR Ott, and G Aeppli. Experimental Perspectives on Heavy-Electron Metals. *Jpn. J. Appl. Phys.*, 26(Part 3 Suppl. 26-3):1882–1886, 1987. Suppl. 26-3.
- [21] K Heuser, EW Scheidt, T Schreiner, and GR Stewart. Inducement of non-Fermi-liquid behavior with a magnetic field. *Phys. Rev. B*, 57(8):R4198–R4201, Feb 1998.
- [22] SL Bud'ko, E Morosan, and PC Canfield. Magnetic field induced non-Fermi-liquid behavior in YbAgGe single crystals. *Phys. Rev. B*, 69(1):014415, Jan 2004.
- [23] T Westerkamp, M Deppe, R KÜchler, M Brando, C Geibel, P Gegenwart, AP Pikul, and F Steglich. Kondo-Cluster-Glass State near a Ferromagnetic Quantum Phase Transition. *Phys. Rev. Lett.*, 102(20):206404, MAY 22 2009.
- [24] AV Chubukov, C Pépin, and J Rech. Instability of the Quantum-Critical Point of Itinerant Ferromagnets. *Phys. Rev. Lett.*, 92(14):147003, Apr 2004.
- [25] M Nicklas, M Brando, G Knebel, F Mayr, W Trinkl, and A Loidl. Non-Fermi-Liquid Behavior at a Ferromagnetic Quantum Critical Point in $\text{Ni}_x\text{Pd}_{1-x}$. *Phys. Rev. Lett.*, 82(21):4268–4271, May 1999.
- [26] DA Sokolov, MC Aronson, W Gannon, and Z Fisk. Critical Phenomena and the Quantum Critical Point of Ferromagnetic $\text{Zr}_{1-x}\text{Nb}_x\text{Zn}_2$. *Phys. Rev. Lett.*, 96(11):116404, Mar 2006.
- [27] S Jia, P Jiramongkolchai, MR Suchomel, BH Toby, JG Checkelsky, NP Ong, and RJ Cava. Ferromagnetic quantum critical point induced by dimer-breaking in $\text{SrCo}_2(\text{Ge}_{1-x}\text{P}_x)_2$. *Nature Phys.*, 7:207–210, 2011.
- [28] T Vojta. Disorder-Induced Rounding of Certain Quantum Phase Transitions. *Phys. Rev. Lett.*, 90(10):107202, Mar 2003.
- [29] S Friedemann, N Oeschler, S Wirth, C Krellner, C Geibel, F Steglich, S Paschen, S Kirchner, and Q Si. Fermi-surface collapse and dynamical scaling near a quantum-critical point. *Proc. Natl. Acad. Sci. USA*, 107(33):14547–14551, AUG 17 2010.
- [30] P Gegenwart, J Custers, Y Tokiwa, C Geibel, and F Steglich. Ferromagnetic Quantum Critical Fluctuations in $\text{YbRh}_2(\text{Si}_{0.95}\text{Ge}_{0.05})_2$. *Phys. Rev. Lett.*, 94(7):076402, Feb 2005.
- [31] C Klingner, C Krellner, M Brando, C Geibel, F Steglich, DV Vyalikh, K Kummer, S Danzenbächer, SL Molodtsov, C Laubschat, T Kinoshita, Y Kato, and T Muro. Evolution of magnetism in $\text{Yb}(\text{Rh}_{1-x}\text{Co}_x)_2\text{Si}_2$. *Phys. Rev. B*, 83:144405, Apr 2011.
- [32] J Custers, P Gegenwart, H Wilhelm, K Neumaier, Y Tokiwa, O Trovarelli, C Geibel, F Steglich, C Pepin, and P Coleman. The break-up of heavy electrons at a quantum critical point. *Nature*, 424:524–527, 2003.
- [33] C Krellner, S Hartmann, A Pikul, N Oeschler, JG Donath, C Geibel, F Steglich, and J Wosnitzer. Violation of Critical Universality at the Antiferromagnetic Phase Transition of YbRh_2Si_2 . *Phys. Rev. Lett.*, 102(19):196402, May 2009.
- [34] K Koepnik and H Eschrig. Full-potential nonorthogonal local-orbital minimum-basis band-structure scheme. *Phys. Rev. B*, 59:1743–1757, JAN 15 1999.
- [35] JP Perdew and Y Wang. Accurate and simple analytic representation of the electron-gas correlation energy. *Phys. Rev. B*, 45:13244–13249, Jun 1992.

- [36] T Sakakibara, H Mitamura, T Tayama, and H Amitsuka. Faraday Force Magnetometer for High-Sensitivity Magnetization Measurements at Very Low Temperatures and High Fields. *Jpn. J. Appl. Phys.*, 33(9A):5067–5072, SEP 1994.
- [37] LG Akselrud, PYu Zavalii, Yu Grin, V Pecharsky, B Baumgartner, and E Wölfel. Use of the CSD Program Package for Structure Determination from Powder Data. *Mater. Sci. Forum*, 133-136:335–340, 1993.
- [38] GM Sheldrick. A short history of SHELX. *Acta Cryst. A*, 64:112–122, 2008.